Inhibition of the proteasome and proteaphagy enhances apoptosis in FLT3-ITD-driven acute myeloid leukemia

Rosa G Lopez-reyes, Grégoire Quinet, Maria Gonzalez-Santamarta, Clément Larrue, Jean-Emmanuel Sarry, Manuel S Rodriguez

▶ **To cite this version:**

Rosa G Lopez-reyes, Grégoire Quinet, Maria Gonzalez-Santamarta, Clément Larrue, Jean-Emmanuel Sarry, et al.. Inhibition of the proteasome and proteaphagy enhances apoptosis in FLT3-ITD-driven acute myeloid leukemia. FEBS Open Bio, 2021, 11 (1), pp.48-60. 10.1002/2211-5463.12950 . hal-03007137

HAL Id: hal-03007137
https://hal.science/hal-03007137v1

Submitted on 16 Nov 2020

HAL is a multi-disciplinary open access archive for the deposit and dissemination of scientific research documents, whether they are published or not. The documents may come from teaching and research institutions in France or abroad, or from public or private research centers.

L'archive ouverte pluridisciplinaire **HAL**, est destinée au dépôt et à la diffusion de documents scientifiques de niveau recherche, publiés ou non, émanant des établissements d'enseignement et de recherche français ou étrangers, des laboratoires publics ou privés.

Check for updates

DR. MANUEL S. RODRIGUEZ (Orcid ID : 0000-0001-5445-4495)

Received Date : 27-May-2020
Revised Date : 15-Jul-2020
Accepted Date : 12-Aug-2020
Article type : Research Article

Inhibition of the proteasome and proteaphagy enhances apoptosis in FLT3-ITD-driven acute myeloid leukemia

Rosa G Lopez-Reyes[1,2], Grégoire Quinet[1], Maria Gonzalez-Santamarta[1], Clément Larrue [2], Jean-Emmanuel Sarry[2], Manuel S. Rodriguez [1].

[1]*Institute of Advanced Technology and Life Sciences (ITAV), IPBS-Centre de la Recherche Scientifique (CNRS), and Université Toulouse III Paul Sabatier, Toulouse France.*

[2]*Cancer Research Center of Toulouse Unité Mixte de Recherche (UMR) 1037 INSERM, ERL 5294 Centre de la Recherche Scientifique (CNRS), Toulouse, France.*

Corresponding authors: Manuel S. Rodriguez, UbiCARE, Institute of Advanced Technology and Life Sciences, 1 Place Pierre Potier, 31000 Toulouse. E-mail: manuel.rodriguez@itav.fr

Running heading: Proteaphagy-inhibition and FLT3-ITD AML apoptosis

Abbreviations: AML, acute myeloid leukaemia; Atg, autophagy; ALS, autophagy-lysosome system; BafA, Bafilomycin A; Bz, Bortezomib; FLT3, fms-like tyrosine kinase 3; LC3B, microtubule-associated proteins 1A/1B light chain 3B; ITD, internal tandem duplication; PI, proteasome inhibitor; TUBEs, tandem ubiquitin bidning entities; UPS, ubiquitin-proteasome system, VT, Verteporfin.

This article has been accepted for publication and undergone full peer review but has not been through the copyediting, typesetting, pagination and proofreading process, which may lead to differences between this version and the Version of Record. Please cite this article as doi: 10.1002/2211-5463.12950

FEBS Open Bio (2020) © 2020 The Authors. Published by FEBS Press and John Wiley & Sons Ltd.

This is an open access article under the terms of the Creative Commons Attribution License, which permits use, distribution and reproduction in any medium, provided the original work is properly cited.

Accepted Article

Abstract: Acute myeloid leukaemia (AML) is a clonal disorder that affects hematopoietic stem cells or myeloid progenitors. One of the most common mutations that results in AML occurs in the gene encoding fms-like tyrosine kinase 3 (*FLT3*). Previous studies demonstrated that AML cells expressing FLT3-ITD are more sensitive to the proteasome inhibitor (PI) Bortezomib (Bz), than FLT3 wild-type cells, and this cytotoxicity is mediated by autophagy. Here we show that proteasome inhibition with Bz results in modest but consistent proteaphagy in MOLM-14 leukemic cells expressing the FLT3-ITD mutation, but not in OCI-AML3 leukemic cells with wild type FLT3. Chemical inhibition of autophagy with Bafilomycin A (BafA) simultaneously blocked proteaphagy and resulted in accumulation of the p62 autophagy receptor in Bz-treated MOLM-14 cells. The use of ubiquitin traps (TUBEs) revealed that ubiquitin plays an important role in proteasome-autophagy crosstalk. The p62 inhibitor Verteporfin (VT) blocked proteaphagy and, importantly, resulted in accumulation of high molecular weight forms of p62 and FLT3-ITD in Bz-treated MOLM-14 cells. Both autophagy inhibitors enhanced Bz-induced apoptosis in FLT3-ITD-driven leukemic cells, underlining the therapeutic potential of these treatments.

Keywords: Proteaphagy, Bortezomib, Ubiquitin, AML, FLT3-ITD, Leukaemia

1. Introduction

Acute myeloid leukaemia (AML) is a clonal disorder that affects hematopoietic stem cells or myeloid progenitors. It is characterized by an accumulation of immature leukemic cells in the bone marrow and peripheral blood and leads to bone marrow failure [1]. AML is a heterogeneous disease with a variety of distinct genetic alterations [2]. One of the most common mutations occurs in the gene encoding fms-like tyrosine kinase 3 (*FLT3*) [3]. This type III receptor tyrosine kinase regulates the normal growth and differentiation of hematopoietic cells via the activation of multiple signalling including Akt, MAPK and Stat5 [4,5]. FLT3 cooperates with other recurrent molecular abnormalities to induce acute leukaemia in preclinical models. Internal tandem duplication (ITD) mutations in the FLT3 gene are found in approximately 30% of AML patients and are associated with a poor clinical outcome. Previous studies demonstrated that AML cells expressing FLT3-ITD are more sensitive to the proteasome inhibitor (PI) Bortezomib (Bz), than FLT3 wild-type cells. This cytotoxicity is mediated by autophagy [6]. Furthermore, the genetic inhibition of early autophagy steps or of autophagosome formation block FLT3-ITD, Stat5 and Akt degradation induced by Bz, [6].

The proteasome has been envisioned as a promising target for the development of anticancer

Accepted Article

therapeutic drugs [7]. The 26S proteasome is a large multi-subunit protease (1500-2000 kDa), formed by the 20S proteolytic core, and one or two 19S regulatory particles [8]. Three proteolytically active subunits integrate the 20S core: β1 with a caspase-like activity, β2 with a trypsin-like activity, and β5 with a chymotrypsin-like activity. β5 is the primary target for most PIs that reached a clinical phase [8,9]. Cancer therapy also targets the Autophagy-Lysosome System (ALS), another proteolytic process that is responsible for the bulk degradation of cytoplasmic components. Amino acid deficiency activates autophagy by regulating signalling cascades controlling this proteolytic pathway [10]. During selective autophagy, phagophores engulf cytoplasmic material, and then fuse to form double-membrane autophagosomes. Cargo recruitment occurs through a family of autophagy receptors including p62, OPTN or NBR1 that are often used as markers for autophagy activation together with the ubiquitin-like molecule Atg8 [11]. The autophagy (Atg) machinery was first identified in yeast and equivalent molecules reported in mammalian cells [11–13]. Distinct autophagy events drive the degradation of organelles or aggregated proteins such as mitophagy (mitochondria), aggrephagy (protein aggregates) or proteasome (proteaphagy), to name a few [14].

Many of the current autophagy inhibitors act at a late stage of the system, such as the V-ATPase inhibitor Bafilomycin A (BafA). BafA inhibits autophagy in a non-selective way, by neutralizing acidic pH of lysosomal hydrolases which drive autophagic degradation [15]. Verteporfin (VT) is an FDA-approved drug that was identified in a screen for chemicals that prevent autophagosome formation [16]. Unlike BafA, VT inhibits autophagy at an early stage, and does not allow autophagosome accumulation[16]. A better understanding of the proteolytic regulation mechanism and interplay will allow exploring alternative/combined treatments to tackle cancer development and/or drug resistance.

Here we aimed to better understand the proteolytic crosstalk connecting proteasome with autophagy after Bz treatment in FLT3-ITD positive MOLM-14 AML cells. Using a chemical approach to block autophagy at distinct levels together with ubiquitin traps (known as TUBEs [17]), immunoprecipitation (IP) and immunofluorescence, we found that proteaphagy was activated after Bz treatment. Although proteaphagy is a process preserved in distinct species [18–20], we found that the presence of FLT3-ITD predisposes MOLM-14 cells to activate it.

2. Material and Methods

Cell lines

Accepted Article

Human myeloid leukaemia cell lines MOLM-14 and OCI-AML-3 were purchased from the ATCC collection. AML cell lines were maintained in RPMI supplemented with 10% foetal calf serum in the presence of 100 U/mL of penicillin and 100 µg/ml of streptomycin. Cells were incubated at 37°C with 5% CO_2[6]. To facilitate autophagy analysis, 2% calf serum was used during chemical inhibitors treatment for a maximum time of 8 hours.

Antibodies and reagents

Antibodies anti-LC3B, anti-Erk 1/2, anti-Stat5, anti-Akt, anti-Ubiquitin (P4D1), anti-PSMB5, were purchased from Cell Signalling Technology (Beverly, MA, USA). Anti-FLT3, anti-p62/SQSTM1 and anti-Beta 2 were obtained from Santa Cruz Biotechnology (Dallas, Texas, USA), anti-PSMA6 from Invitrogen. Anti-PSMB6 and anti-Rpn10 were purchased from Enzo, anti-PSMD3 from Thermofisher and anti-GAPDH from Sigma.

Bortezomib and Chloroquine were purchased from Sigma-Aldrich and Bafilomycin A from InvivoGen, and Verteporfin from Sigma Aldrich.

Western blot analysis

Proteins were resolved using 8 to 12% PAGE and electro-transferred to PVDF membranes. Membranes were then blocked with 5% skimmed powdered milk in TBS, or 5% bovine serum albumin in TBS. Membranes were immunostained with appropriate antibodies and horseradish peroxidase-conjugated secondary antibodies and visualized with enhanced chemiluminescence system.

Apoptosis assay

Cells line were cultured in RPMI 5%, treated at different times with Bortezomib, Bafilomycin A and Verteporfin. Then $5x10^5$ cells were washed with PBS and resuspended in 100 µL of Annexin-V binding buffer. Two microliters of Annexin-V-FITC were added at room temperature. All samples were analysed by a fluorescent-activated cell sorter FACS Calibur flow cytometer [6].

TUBES capture

TUBEs were produced according to Hjerpe et al., [17,21]. 20 millions of cells were used for each condition (TUBE p62, TUBE HHR23 or GST Control). Cells were resuspended in 500 µL of TUBE lysis buffer, kept 10 minutes at 4ºC and spin down at 15500 g. A fraction of this supernatant was diluted in 3X boiling buffer (50 mM Tris-HCl, pH 6.8, 10% glycerol, 2% SDS, bromophenol blue, 10% β-mercaptoethanol) and considered as Input. Supernatant was transferred to the glutathione-agarose beads with TUBEs or GST control, and samples were incubated overnight in rotation at 4ºC. On the next day, samples were spin down at 500g at 4ºC, a fraction

Accepted Article

recollected, diluted in BB and considered as Flow-throw (FT). Beads were washed 3 times with 1 mL of PBS Tween 0.05%. Beads were resuspended in 100 µL of BB and boiled 5 minutes before protein electrophoresis.

Antibody crosslinking

Thirty microliters per point of magnetic beads protein A (Milipore) were washed with PBS and equilibrated in binding buffer (50mM Tris pH 8.5, 150mM NaCl, + 0.5% NP40), using a magnetic holder. Antibodies were added to beads and rotated overnight. On the next day 10-20 µL of supernatant were kept to control antibody binding. Beads were washed twice with PBS and once with 500 µL of coupling buffer (200mM Borate, 3M NaCl pH9). Fifty millimolar DMP were added to coupling buffer, and samples were rotated during 30 minutes with this crosslinking solution (CS). Supernatant was discarded, replaced with fresh CS and incubated at 4ºC during 30 minutes. Beads were washed twice with coupling buffer before blocking with 20 mM ethanolamine pH 8.2. Supernatant was discarded and replaced by fresh ethanolamine and incubated for an hour. Beads were washed twice with PBS. Non-coupled antibodies were removed with 2 washes of 1M NaCl/binding buffer. A PBS equilibration was done before washing 3 times with 200 mM glycine pH 2.5. Beads were blocked with 0.1% BSA in binding buffer during 90 minutes. Magnetic beads were equilibrated in binding buffer and kept in PBS until used. A fraction of these beads (10-20 µL) were analyzed by electrophoresis followed by Coomassie blue staining to compare antibodies before and after crosslinking.

Immunoprecipitation in presence of TUBEs

Twenty millions of cells were spin down at 300g/10min, the dry pellet was resuspended in 500 µL of TUBE lysis buffer including 100 µg of TUBE p62 or TUBE HHR23[17]. Cell lysates were homogenized with 40 strokes at 4ºC using a dounce homogenizer. The whole sample was centrifuged at 200g/5min and supernatant was recovered for immunoprecipitation. A fraction (1/20) of the supernatant was considered as Input. The crosslinked antibody was incubated with cell lysates in rotation during 1h30 at 4ºC. Samples were disposed in magnetic holder to separate bound from unbound material. Proteins unbound to crosslinked antibodies were considered as flow-through (FT) fraction. Magnetic beads were washed with PBS/tween 0.05% 3-5 times and resuspended in 30 µL BB 3x to be analyzed by Western blot.

Statistical analysis

Data from 4 independent experiments were reported as the mean ± standard error of the mean.

Accepted Article

Statistical analyses were performed using unpaired two-tailed Student *t*-tests with Prism 4 software. P<0.05 was regarded as significant. *, **, ***, **** correspond to P<0.05, P<0.01, P<0.001 and P<0.0001 respectively.

3. Results

Proteaphagy activation after proteasome inhibition in FLT3-ITD mutant driven MOLM-14 leukemic cells

To mechanistically understand the regulation of the crosstalk between UPS and ALS in leukaemia, we investigated the role of proteaphagy which is known to be activated after proteasome inhibition [22]. The impact of Bz was assessed in MOLM-14 cells with the FLT3-ITD mutation and compared with the FLT3 wild-type cell line OCI-AML3 (Fig. 1). Bz treatment does not always promote an obvious degradation of proteasome subunits since proteolysis can be compensated by the *novo* synthesis of these subunits as previously reported [23,24]. For this reason, proteaphagy was evaluated by the degradation of 20S and 19S proteasomal subunits after Bz treatment and their accumulation with autophagy inhibitors. BafA treatment resulted in the accumulation of autophagy markers p62 and LC3B in the presence or absence of Bz, indicating that autophagy was activated under these experimental conditions in both cell lines (Fig. 1A). Nevertheless, lipidated forms of LC3B were only observed after BafA treatment in MOLM-14 but not in OCI-AML3. The low levels of apoptosis observed after 8h of individual or combined Bz/BafA treatment excluded the possibility that differences could be due to massive death of MOLM-14 cells (Fig. S1). Our results showed a modest but consistent Bz-mediated degradation of 20S proteasome subunits α6s and β5 and 19S subunits Rpn1 and Rpn3 that was blocked by BafA in MOLM-14 (Fig. 1B and C). However, the combination of BafA with Bz did not significantly accumulate proteasome subunits in OCI-AML3 as it was the case in MOLM-14 cells (Fig. 1B and C low panels), suggesting that a predisposition for degradation of 26S proteasome could be linked to the presence of FLT3-ITD. These results were also confirmed by immunofluorescence where proteasomes subunit β2 or α2 colocalized with autophagosomes (Atg8 equivalent LC3B or p62 staining respectively) after Bz/BafA treatment of MOLM-14 cells (Fig. 2A and B). This Bz-induced degradation of proteasome subunits is blocked by BafA, indicating that proteaphagy mediated these proteolytic events.

Role of p62 and ubiquitin in Bz-induced autophagy

To analyse the role of p62 in the Bz-induced autophagic degradation of the proteasomes and

Accepted Article

FLT3-ITD, the interaction of p62 with proteasome subunits and FLT3-ITD was investigated. IP experiments using a specific p62 antibody were performed using MOLM-14 cells treated or not with Bz/BafA. Taking advantage of the protective effects of TUBEs that block the action of proteases, accumulate ubiquitylated proteins and interact with multiple chain types [17,25], IPs were done in the presence or absence of TUBEs based in the UBA domain of HHR23 (TUBE-HHR23) or the UBA domain of p62 (TUBE-p62) (Fig. 3A). In the absence of TUBEs, p62 was immunoprecipitated without treatment and Bz/BafA reduced the level of precipitated p62. However, in the presence of both TUBEs, p62 was protected from proteasome and/or autophagy mediated degradation under Bz/BafA conditions (Fig. 3A). Compared to the situation without any TUBEs or TUBE-HHR23, the presence of TUBE-p62 allows a better coimmunoprecipitation of p62-bound proteasome subunits β2 and but not RPN1. High molecular weight forms most likely representing ubiquitylated forms of RPN1 were better immunoprecipitated in the presence of TUBE-HHR23 (Fig. 3A). Consistent with these observations, FLT3-ITD was also protected by TUBE-p62 but putative ubiquitylated forms of this protein were better immunoprecipitated in the presence of TUBE-HHR23.

Since ubiquitin is a major coordinator of UPS and ALS, we investigated its role in the crosstalk of these pathways induced after Bz and BafA treatments. In particular, we were interested in investigating whether the high molecular weight forms of FLT3 co-immunoprecipitated with p62 corresponded to ubiquitylated FLT3. TUBE-HHR23 was used to capture total ubiquitylated proteins from MOLM-14 cells treated or not with individual and combined Bz/BafA treatment (Fig. 3B). Total ubiquitylated proteins were efficiently trapped by TUBE-HHR23. BafA treatment alone did not significantly enrich ubiquitylated proteins captured by TUBE-HHR23 compared to Bz or Bz/BafA. Proteasome subunits β5 and Rpn1 are captured by TUBE-HHR23 (Fig. 3B). The p62 receptor was also captured under the same conditions but the combination of Bz/BafA enriched this protein compared to Bz alone (Fig. 3B). Interestingly, ubiquitylated forms of FLT3-ITD were captured by TUBE-HHR23 under all conditions but best enriched when Bz/BafA treatment was used (Fig. 3B).

p62 drives proteaphagy and autophagic degradation of FLT3-ITD

To further assess the role of the autophagy receptor p62 in proteaphagy, VT was used to treat MOLM-14 cells and Western blot analyses were performed to detect distinct proteasome subunits. High molecular weight forms of p62 were detected after VT treatment (Fig. 4A). Interestingly, the lipidated form of LC3B decreases after VT treatment, indicating that this drug reduced the

Accepted Article

autophagy flux. Bz-mediated degradation of 20S or 19S subunits was blocked by VT even if the Bz-mediated degradation of 19S subunits was more prominent than 20S subunits (Fig. 4B and C). The colocalization of p62/α_2 was significantly reduced with VT or Bz/VT indicating that blocking of p62 could inhibit proteaphagy through a mechanism distinct from BafA (Fig. 4D). To investigate if the high molecular weight forms of p62 observed in Fig 4A were aggregated and/or ubiquitylated, IP were performed with p62 antibodies in the presence or absence of TUBE-p62 (Fig 4E) and TUBE-capture of ubiquitylated proteins (Fig. 4F). Interestingly, the aggregated forms of p62 generated after the Bz/VT treatment do not interact with the lipidated form of LC3B indicating that this treatment negatively affected this interaction (Fig. 4E). The lipidated forms of LCB3 were also reduced in the input fraction indicating that VT stops the autophagy flux as it was observed in Figure 4A. In order to explore the ubiquitylation status of p62 after VT treatment we captured ubiquitylated proteins using TUBE-p62 (Figure 4F). VT has a negative impact on the total ubiquitylated proteins as it can be observed in the input fraction. Nevertheless, the levels of ubiquitylation could be recovered when VT was combined with Bz. These results were also observed in the TUBE capture of total ubiquitylated proteins. Under these experimental conditions, p62 increased its ubiquitylated levels after Bz treatment and decreased when cells were treated with VT (Figure 4F). Altogether these evidences indicated that after VT treatment, aggregated forms of p62 are accumulated and these forms are less ubiquitylated. The reduction of the interaction p62/lipidated LC3B indicate that this p62 was not integrated into autophagosomes after Bz/VT treatment. In a similar manner, VT reduced the localization of p62 with proteasome subunits, supporting the notion that proteaphagy is hampered by this treatment (Figure 4D). Thus, these data show that p62 plays an important role in proteaphagy observed in MOLM-14 cells.

Inhibition of UPS and ALS pathways enhances apoptosis of FLT3-ITD cells

Individual or combined treatments were used to investigate if Bz-induced degradation of FLT3-ITD was blocked by VT in MOLM-14 cells (Fig 5A). Our results indicate that FLT3-ITD and FLT3 were degraded up to 25% after Bz treatment in MOLM-14 cells (Fig 5A). FLT3-ITD degradation was blocked by VT while high molecular weight forms of FLT3 were formed under the same conditions in MOLM-14 suggesting a ubiquitin driven autophagy-mediated proteolysis event (Fig. 5A). Interestingly, in OCI-AML3 cells, under the same experimental conditions FLT3 was not degraded by Bz and VT treatment rather accumulated high mobility forms of this protein (Fig. 5B). The double Bz/VT treatment does not significantly accumulate FLT3 in OCI-AML3

Accepted Article

(Fig. 5B), supporting the notion that proteolytic pathways are not efficiently activated in these cells.

Finally, we investigated the consequences of accumulated proteasome and FLT3-ITD after inhibition of UPS and ALS pathways in MOLM-14 cells and compared to OCI-AML3 cells. Apoptosis was measured by analysing Annexin-V positive cells after single agent or combined treatments (Fig. 5). Bz-induced cell death was always kept below 50% to differentiate positive or negative effects of BafA on the Bz treatments. To improve the efficiency of autophagy inhibition, cells were pre-treated 8h with BafA before adding Bz for an additional 16h at the indicated doses (Fig. 5C and D). Our results showed that the toxicity of the individual BafA treatment was around 20% (MOLM-14) or below 5% (OCI-AML3) and both drugs efficiently cooperated to enhance the cell killing effect on MOLM-14 (Fig. 5C) but this was not in the case in OCI-AML3 (Fig. 5D). Apoptosis induced by VT also improved the results observed with Bz alone in MOLM-14 cells (Fig. 5E) but not in OCI-AML3 cells (Fig. 5F). In this case, Bz and VT were simultaneously added to cell cultures to work below the VT IC50. This results in an additional 8h of Bz compared to Fig. 5A, explaining the higher apoptosis observed with Bz treatment only. Cooperative effects observed with the double Bz/VT treatment were statistically significant in MOLM-14 cells but not in OCI-AML3 (Fig. 5E and 5F). Altogether, our results show that the inhibition of both proteolytic pathways markedly enhances apoptosis levels in MOLM-14 that express FLT3-ITD (Fig. 6) but not in OCI-AML3 that express WT FLT3.

4. Discussion

Multiple mechanisms of interplay between the UPS and ALS have been documented over the last ten years. Here we identified proteaphagy as part of the selective autophagic events, which are activated after Bz treatment in FLT3-ITD positive leukemic cells. Our data showed that this tyrosine kinase translocation facilitates the Bz-mediated proteolysis of 20S and 19S subunits and their colocalization within autophagosomes. FLT3-ITD can potentially predispose to proteaphagy due to its capacity to activate multiple signalling cascades that have an impact on autophagy activation. Among these pathways are the phosphatidylinositol-3 kinase (PI3K) [26,27], Akt [28], mammalian target of rapamycin (mTOR) [29], RAS, and extracellular signal-related kinase (Erk), MAPK and Stat5 [5,30]. It remains to be demonstrated if any or various of these signalling pathways have a positive or negative impact on proteaphagy.

Proteaphagy is a complicated process to analyse since not all proteasomes are directly concerned

Accepted Article

by this type of degradation. Nuclear proteasomes will not be immediately affected since proteaphagy is a cytoplasmic event. According to the literature, only 20-50% of the proteasomes are regulated by proteaphagy depending on the time, intensity and type of stimuli in distinct biologic models [18–20]. Our results demonstrate that the autophagy receptor p62 is implicated in the proteaphagy activated by Bz in MOLM-14 cells. However, our data do not exclude the participation of other autophagy receptors in this process [14]. For instance, both the ubiquitin receptor Cue5 and the chaperon Hsp40 [19] or the proteasome subunit RPN10 [18], respectively mediate proteaphagy in *Saccharomyces cerevisiae* or *Arabidopsis thaliana*. Nevertheless, the use of VT in leukemic cells showed that the inactivation of p62 stops Bz-induced proteaphagy supporting a major role of p62 in this process. Interestingly, VT favours the formation of high molecular weight aggregates of p62 [31], which are also observed with FLT3-ITD with the same treatment. However, other effects have been reported for VT including the activation of ROS that could affect other processes [32,33] making difficult to attribute VT effects only to its action on p62.

The IP/protection assays [17] revealed that TUBE-p62 protects p62, RPN1, β2 or FLT3-ITD from Bz-driven degradation blocked with BafA in MOLM14 cells. TUBE-HHR23 also protects these factors but to a lesser extent than TUBE-p62. However, TUBE-HHR23 better accumulates ubiquitylated forms of RPN1 or FLT3-ITD. Similar IP experiments performed with Bz/VT in MOLM-14 showed that high molecular weight forms of p62 did not interact with the lipidated form of LC3B, indicating that p62 was not integrated into autophagosomes under those conditions. This could be associated to the reduction of total ubiquitylated forms observed after VT treatment that might have a negative impact in ubiquitin-regulated events.

The ubiquitin proteome captured with TUBE-HHR23 includes several proteins implicated in proteaphagy such as p62, RPN1 or β5 after Bz or Bz/BafA treatments but not with BafA alone, indicating that this autophagy inhibitor does not accumulate ubiquitylated forms of these factors in the absence of proteasome inhibition. TUBE-p62 captures significantly less ubiquitylated proteins than TUBE-HHR23 and specific ubiquitylated forms can only be seen when overexposing. Nonetheless, in this way we found that while Bz accumulated ubiquitylated forms of p62, VT reduces these forms most likely interfering with the integration of this receptor into autophagosomes. The use of both TUBEs to investigate UPS and ALS regulated events has the interest to keep all possibilities open to find which pathway will be playing a role under distinct experimental settings. While TUBE-HHR23 recognises virtually all types of chains [17,34,35], the

Accepted Article

UBA domain of p62 recognises mainly K63 ubiquitin chains explaining the observed differences [36,37].

Altogether our data indicate that when both proteolytic pathways are blocked, accumulation of cellular factors occurs due to the functional absence of these degradation machineries (Fig. 6). This contributes to enhance apoptosis in MOLM-14 but not OCI-AML3 cells under the same experimental conditions. In conclusion, targeting protein homeostasis could be an alternative to improve current treatments of FLT3-ITD AML cells. Although the crosstalk of these complex proteolytic mechanisms remains to be fully elucidated, our results open new possibilities for the treatment of this AML phenotype.

Acknowledgments

We thank Clémence Coutelle-Rebut for the proofreading of this manuscript. MSR and MGS are funded by UbiCODE a network supported by the European Union's Horizon 2020 research and innovation programme under the Marie Skłodowska-Curie grant agreement No 765445. MSR also receives funding from the Institut National du Cancer, France (PLBIO16-251), LASSERLAB-EUROPE under the grant No 654148, CONACyT-SRE (Mexico) under the grant No 0280365 and the Occitanie region, France, through the REPERE and Prematuration programs. GQ and RGLR are respectively fellows from The French Ministry of Higher Education and Research and CONACYT (Mexico).

Author Contributions

RGLP, MSR, JES conceived and designed the project, RGLP, GQ and MGS acquired the data, RGLP, GQ, MGS and CL analysed and interpreted the data, MSR and RGLP wrote the paper, all authors contributed to proofread this manuscript.

Data Accessibility

Data will be available from the corresponding author upon reasonable request.

Conflict of interest

Authors declare no conflict of interest.

References

1 Horton SJ & Huntly BJP (2012) Recent advances in acute myeloid leukemia stem cell biology. *Haematologica* **97**, 966–974.

Accepted Article

Accepted Article

2 Staudt D, Murray HC, McLachlan T, Alvaro F, Enjeti AK, Verrills NM & Dun MD (2018) Targeting Oncogenic Signaling in Mutant FLT3 Acute Myeloid Leukemia: The Path to Least Resistance. *Int J Mol Sci* **19**.

3 Pratz KW & Luger SM (2014) Will FLT3 Inhibitors Fulfill Their Promise in AML? *Curr Opin Hematol* **21**, 72–78.

4 Takahashi S (2011) Downstream molecular pathways of FLT3 in the pathogenesis of acute myeloid leukemia: biology and therapeutic implications. *J Hematol OncolJ Hematol Oncol* **4**, 13.

5 Choudhary C, Müller-Tidow C, Berdel WE & Serve H (2005) Signal transduction of oncogenic Flt3. *Int J Hematol* **82**, 93–99.

6 Larrue C, Saland E, Boutzen H, Vergez F, David M, Joffre C, Hospital M-A, Tamburini J, Delabesse E, Manenti S, Sarry JE & Récher C (2016) Proteasome inhibitors induce FLT3-ITD degradation through autophagy in AML cells. *Blood* **127**, 882–892.

7 Liu Y, Huang W-J, Lin M-T, Li J-J & Zhang J-Y (2019) Chapter 13 - Proteasome Inhibitors as Sensitizing Agents for Cancer Chemotherapy. In *Protein Kinase Inhibitors as Sensitizing Agents for Chemotherapy* (Chen Z-S & Yang D-H, eds), pp. 207–228. Academic Press.

8 Finley D, Chen X & Walters KJ (2016) Gates, Channels, and Switches: Elements of the Proteasome Machine. *Trends Biochem Sci* **41**, 77–93.

9 Orlowski M & Wilk S (2000) Catalytic activities of the 20 S proteasome, a multicatalytic proteinase complex. *Arch Biochem Biophys* **383**, 1–16.

10 Mejlvang J, Olsvik H, Svenning S, Bruun J-A, Abudu YP, Larsen KB, Brech A, Hansen TE, Brenne H, Hansen T, Stenmark H & Johansen T (2018) Starvation induces rapid degradation of selective autophagy receptors by endosomal microautophagy. *J Cell Biol* **217**, 3640–3655.

11 Rogov V, Dötsch V, Johansen T & Kirkin V (2014) Interactions between autophagy receptors and ubiquitin-like proteins form the molecular basis for selective autophagy. *Mol Cell* **53**, 167–178.

12 Kraft C, Peter M & Hofmann K (2010) Selective autophagy: ubiquitin-mediated recognition and beyond. *Nat Cell Biol* **12**, 836–841.

13 Mizushima N, Yoshimori T & Ohsumi Y (2011) The Role of Atg Proteins in Autophagosome Formation. *Annu Rev Cell Dev Biol* **27**, 107–132.

FEBS Open Bio (2020) © 2020 The Authors. Published by FEBS Press and John Wiley & Sons Ltd.

Accepted Article

14 Mancias JD & Kimmelman AC (2016) Mechanisms of selective autophagy in normal physiology and cancer. *J Mol Biol* **428**, 1659–1680.

15 Juhász G (2012) Interpretation of bafilomycin, pH neutralizing or protease inhibitor treatments in autophagic flux experiments: novel considerations. *Autophagy* **8**, 1875–1876.

16 Donohue E, Tovey A, Vogl AW, Arns S, Sternberg E, Young RN & Roberge M (2011) Inhibition of autophagosome formation by the benzoporphyrin derivative verteporfin. *J Biol Chem* **286**, 7290–7300.

17 Hjerpe R, Aillet F, Lopitz-Otsoa F, Lang V, England P & Rodriguez MS (2009) Efficient protection and isolation of ubiquitylated proteins using tandem ubiquitin-binding entities. *EMBO Rep* **10**, 1250–1258.

18 Marshall RS, Li F, Gemperline DC, Book AJ & Vierstra RD (2015) Autophagic Degradation of the 26S Proteasome Is Mediated by the Dual ATG8/Ubiquitin Receptor RPN10 in Arabidopsis. *Mol Cell* **58**, 1053–1066.

19 Marshall RS, McLoughlin F & Vierstra RD (2016) Autophagic Turnover of Inactive 26S Proteasomes in Yeast Is Directed by the Ubiquitin Receptor Cue5 and the Hsp42 Chaperone. *Cell Rep* **16**, 1717–1732.

20 Cohen-Kaplan V, Livneh I, Avni N, Fabre B, Ziv T, Kwon YT & Ciechanover A (2016) p62- and ubiquitin-dependent stress-induced autophagy of the mammalian 26S proteasome. *Proc Natl Acad Sci* **113**, E7490–E7499.

21 Aillet F, Lopitz-Otsoa F, Hjerpe R, Torres-Ramos M, Lang V & Rodríguez MS (2012) Isolation of ubiquitylated proteins using tandem ubiquitin-binding entities. *Methods Mol Biol Clifton NJ* **832**, 173–183.

22 Waite KA, Mota-Peynado AD-L, Vontz G & Roelofs J (2016) Starvation Induces Proteasome Autophagy with Different Pathways for Core and Regulatory Particles. *J Biol Chem* **291**, 3239–3253.

23 Meiners S, Heyken D, Weller A, Ludwig A, Stangl K, Kloetzel P-M & Krüger E (2003) Inhibition of proteasome activity induces concerted expression of proteasome genes and de novo formation of Mammalian proteasomes. *J Biol Chem* **278**, 21517–21525.

24 Welk V, Coux O, Kleene V, Abeza C, Trümbach D, Eickelberg O & Meiners S (2016) Inhibition of Proteasome Activity Induces Formation of Alternative Proteasome Complexes. *J Biol Chem* **291**, 13147–13159.

FEBS Open Bio (2020) © 2020 The Authors. Published by FEBS Press and John Wiley & Sons Ltd.

Accepted Article

25 Altun M, Kramer HB, Willems LI, McDermott JL, Leach CA, Goldenberg SJ, Kumar KGS, Konietzny R, Fischer R, Kogan E, Mackeen MM, McGouran J, Khoronenkova SV, Parsons JL, Dianov GL, Nicholson B & Kessler BM (2011) Activity-based chemical proteomics accelerates inhibitor development for deubiquitylating enzymes. *Chem Biol* **18**, 1401–1412.

26 Piddock RE, Bowles KM & Rushworth SA (2017) The Role of PI3K Isoforms in Regulating Bone Marrow Microenvironment Signaling Focusing on Acute Myeloid Leukemia and Multiple Myeloma. *Cancers* **9**, 29.

27 Nepstad I, Hatfield KJ, Grønningsæter IS & Reikvam H (2020) The PI3K-Akt-mTOR Signaling Pathway in Human Acute Myeloid Leukemia (AML) Cells. *Int J Mol Sci* **21**, 2907.

28 Brandts CH, Sargin B, Rode M, Biermann C, Lindtner B, Schwäble J, Buerger H, Müller-Tidow C, Choudhary C, McMahon M, Berdel WE & Serve H (2005) Constitutive activation of Akt by Flt3 internal tandem duplications is necessary for increased survival, proliferation, and myeloid transformation. *Cancer Res* **65**, 9643–9650.

29 Tabe Y, Tafuri A, Sekihara K, Yang H & Konopleva M (2017) Inhibition of mTOR kinase as a therapeutic target for acute myeloid leukemia. *Expert Opin Ther Targets* **21**, 705–714.

30 Spiekermann K, Bagrintseva K, Schwab R, Schmieja K & Hiddemann W (2003) Overexpression and constitutive activation of FLT3 induces STAT5 activation in primary acute myeloid leukemia blast cells. *Clin Cancer Res Off J Am Assoc Cancer Res* **9**, 2140–2150.

31 Konstantinou EK, Notomi S, Kosmidou C, Brodowska K, Al-Moujahed A, Nicolaou F, Tsoka P, Gragoudas E, Miller JW, Young LH & Vavvas DG (2017) Verteporfin-induced formation of protein cross-linked oligomers and high molecular weight complexes is mediated by light and leads to cell toxicity. *Sci Rep* **7**, 46581.

32 Lefaki M, Papaevgeniou N & Chondrogianni N (2017) Redox regulation of proteasome function. *Redox Biol* **13**, 452–458.

33 Finkel T (2011) Signal transduction by reactive oxygen species. *J Cell Biol* **194**, 7–15.

34 Altun M, Kramer HB, Willems LI, McDermott JL, Leach CA, Goldenberg SJ, Kumar KGS, Konietzny R, Fischer R, Kogan E, Mackeen MM, McGouran J, Khoronenkova SV, Parsons JL, Dianov GL, Nicholson B & Kessler BM (2011) Activity-based chemical

proteomics accelerates inhibitor development for deubiquitylating enzymes. *Chem Biol* **18**, 1401–1412.

35 Xolalpa W, Mata-Cantero L, Aillet F & Rodriguez MS (2016) Isolation of the Ubiquitin-Proteome from Tumor Cell Lines and Primary Cells Using TUBEs. *Methods Mol Biol Clifton NJ* **1449**, 161–175.

36 Long J, Gallagher TRA, Cavey JR, Sheppard PW, Ralston SH, Layfield R & Searle MS (2008) Ubiquitin Recognition by the Ubiquitin-associated Domain of p62 Involves a Novel Conformational Switch. *J Biol Chem* **283**, 5427–5440.

37 Cabe M, Rademacher DJ, Karlsson AB, Cherukuri S & Bakowska JC (2018) PB1 and UBA domains of p62 are essential for aggresome-like induced structure formation. *Biochem Biophys Res Commun* **503**, 2306–2311.

Figure legends

Fig. 1. Bz-driven proteaphagy is enhanced in FLT3-ITD phenotype. MOLM-14 (FLT3-ITD+/-) or OCI-AML3 (FLT3-WT) cells were treated 8h with Bz 10 nM, and 20 nM Bafilomycin. Total cell lysates were resolved by SDS-PAGE and immunoblotted with the indicated antibodies recognizing the autophagy receptor p62 (A), proteasome core subunits α6 and β5 (B) or 19S subunits Rpn1 and Rpn3 (C). Protein expression levels were quantified by densitometry analysis (Image J software). Statistical analyses were performed using unpaired two-tailed Student *t*-tests with Prism 4 software. P<0.05 was regarded as significant. *, **, ***, **** correspond to P<0.05, P<0.01, P<0.001, P<0.0001 respectively, the data are the s.e.m, n=4.

Fig. 2. Colocalization of proteasome and autophagy markers after Bz and autophagy inhibitors treatment in FLT3-ITD AML cells. Indirect immunofluorescence staining LC3B/β_2 (A) or p62/ α_2 (B) positive structures in MOLM-14 cells treated 8h with Bz 10 nM and 20 nM BafA. Images were captured by confocal microscopy. Scale bar 10 μm Immunofluorescence images were quantified from 3 replicates. Statistical analyses were performed using unpaired two-tailed Student t-tests with Prism 6 software. P<0.05 was regarded as significant. *, **, ***, **** correspond to P<0.05, P<0.01, P<0.001, P<0.0001 respectively, the data are the s.e.m.

Fig. 3. Ubiquitin role in proteaphagy and degradation of FLT3-ITD under proteasome inhibition conditions. MOLM-14 cells were treated or not during 8h with Bz 10 nM, BafA 20 nM

Accepted Article

or both drugs and cells were lysed as reported [17]. Ubiquitylated proteins were captured using TUBEs-HHR23, TUBEs-p62 or GST control (A). Captured proteins were resolved is SDS-PAGE and immunoblotted with the indicated antibodies. Input and flow through (FT) fractions were also analysed with anti-ub antibody. GAPDH was used as loading control. (B) MOLM-14 cells were treated or not with Bz/BafA under the same conditions than "A". p62-bound proteins were captured by IP with a specific p62 antibody in the presence or absence of TUBE-HHR23 or TUBE-p62. Precipitated material was analysed by Western-blot with the indicated antibodies. Input fraction was analysed for the indicated proteins.

Fig. 4. p62 drives proteaphagy in FLT3-ITD AML cells. MOLM-14 cells were treated 8h with Bz 10 nM and VT 1μM. Total cell lysates were resolved by SDS-PAGE and immunoblotted with antibodies against autophagy markers LCB3 and p62 (A), proteasome core subunits α6 and β5 (B) and 19 subunits Rpn1 and Rpn3 (C). Protein expression levels were quantified by densitometry analysis (Image J software). (D) Indirect immunofluorescence staining of p62/ α_2 positive structures in MOLM-14 cells treated 8h with Bz 10 nM and 1 μM VT. Images were captured by confocal microscopy. Scale bar 10 μm. Immunofluorescence images were quantified from 3 replicates. Statistical analyses were performed using unpaired two-tailed Student t-tests with Prism 6 software. $P<0.05$ was regarded as significant. *, **, ***, **** correspond to $P<0.05$, $P<0.01$, $P<0.001$, $P<0.0001$ respectively, the data are the s.e.m. n=5. (E) Immunoprecipitation of p62 from MOLM-14 cells treated or not with Bz 10nM and VT 1μM. Experiments were performed in the presence or absence of TUBE-p62. Precipitated material was analysed by Western blot with specific p62 and LC3B antibodies. Input fraction was analysed with the indicated antibodies. (F) Capture of ubiquitylated proteins using TUBE-p62 trap. GST was used as negative control. Captured proteins were analysed by Western blot with anti-ubiquitin or p62 antibodies. Input and flow through (FT) fractions were analysed with the indicated antibodies.

Fig. 5. Proteasome and autophagy inhibitors cooperate to improve apoptosis of FLT3-ITD expressing cells. MOLM-14 (A) and OCI-AML3 (B) cells were treated 8h with Bz 10 nM and VT 1μM. Total cell lysates were resolved by SDS-PAGE and immunoblotted with antibodies against FLT3 (A and B). Protein expression levels were quantified by densitometry analysis (Image J software). Statistical analyses were performed using unpaired two-tailed Student t-tests with Prism

Accepted Article

6 software. P<0.05 was regarded as significant. *, **, ***, **** correspond to P<0.05, P<0.01, P<0.001, P<0.0001 respectively, the data are the s.e.m. (C and D) MOLM-14 and OCI-AML3 cells were treated 8h with BafA 15nM. Bz was added at 6 or 7.5 nM concentration for additional 16h. (E and F) MOLM-14 and OCI-AML3 cells were treated with a fixed concentration of Bz 7.5 nM and two distinct doses of VT (0.5 and 1 μM) as indicated. Apoptosis was analysed in by FACS. Percentage of cell death was measured from 4 biological replicates. Statistical analyses were performed using unpaired two-tailed Student *t*-tests with Prism 4 software. P<0.05 was regarded as significant. *, **, ***, **** correspond to P<0.05, P<0.01, P<0.001, P<0.0001 respectively, the data are the s.e.m, n=3.

Fig. 6. UPS and ALS crosstalk under proteasome and/or autophagy inhibition. 1) Under basal unstimulated conditions, turnover of important cellular factor is ensured by equilibrated proteolytic pathways 2) Inhibition of proteasome directs crucial cellular factors to ALS for degradation. 3) Autophagy inhibition drives the degradation of some cellular factors to proteasome-mediated degradation 4) when both proteolytic pathways are impaired, both UPS and ALS contribute to accumulate cellular factors and increase apoptosis in FLT3-ITD positive cells.

Supporting Information

Supplementary Fig 1. Cell death evaluation at 8h. Treatments using Bz 15 nM and BafA 10 nM with FBS 2% MOLM-14 before Annexin-V staining and flow cytometry, to validate Western blot conditions N= 24, 3 biological replicates. Statistical analyses were performed using unpaired two-tailed Student t-tests with Prism 6 software. P<0.05 was regarded as significant. *, **, ***,**** correspond to P<0.05, P<0.01, P<0.001, P<0.0001 respectively, the data are the s.e.m, n=3.

Accepted Article

Accepted Article

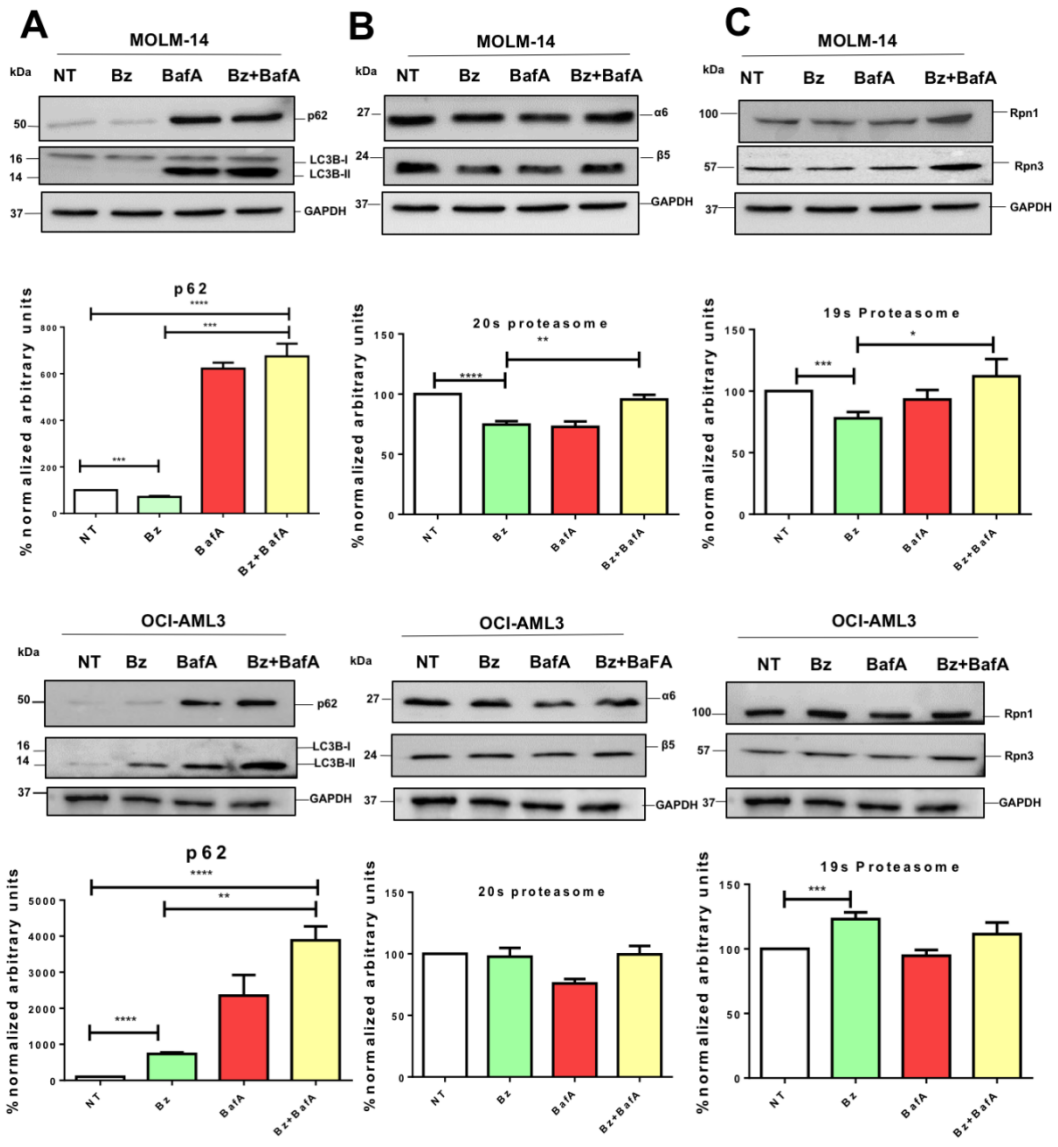

FIGURE 1

feb4_12950_f1.tiff

FEBS Open Bio (2020) © 2020 The Authors. Published by FEBS Press and John Wiley & Sons Ltd.

Accepted Article

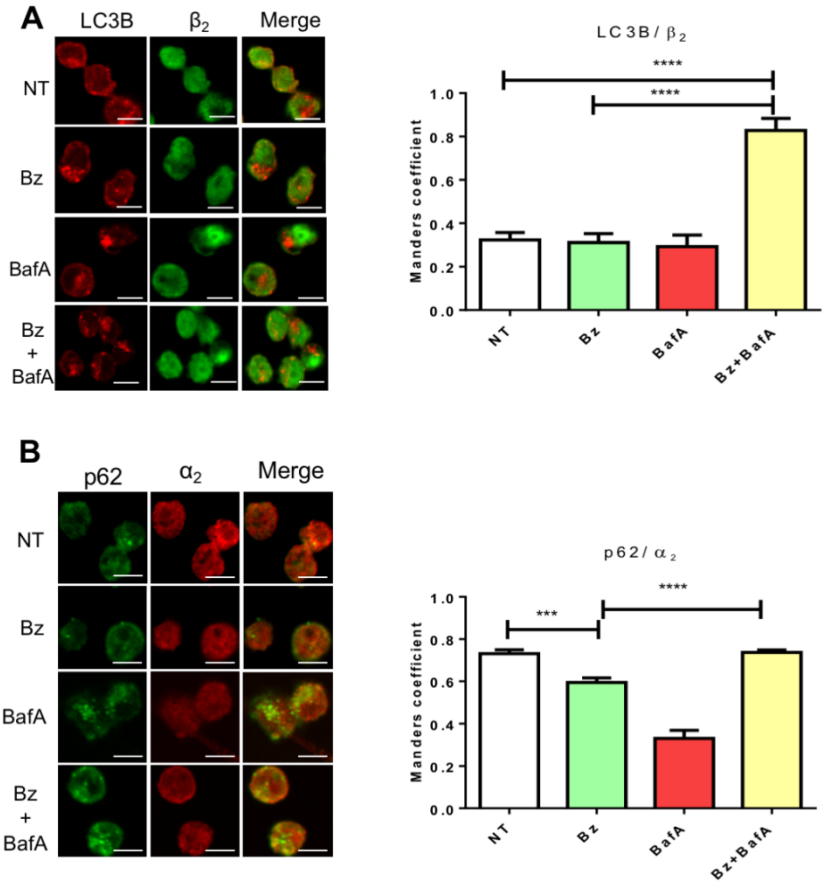

FIGURE 2

feb4_12950_f2.tiff

FEBS Open Bio (2020) © 2020 The Authors. Published by FEBS Press and John Wiley & Sons Ltd.

Accepted Article

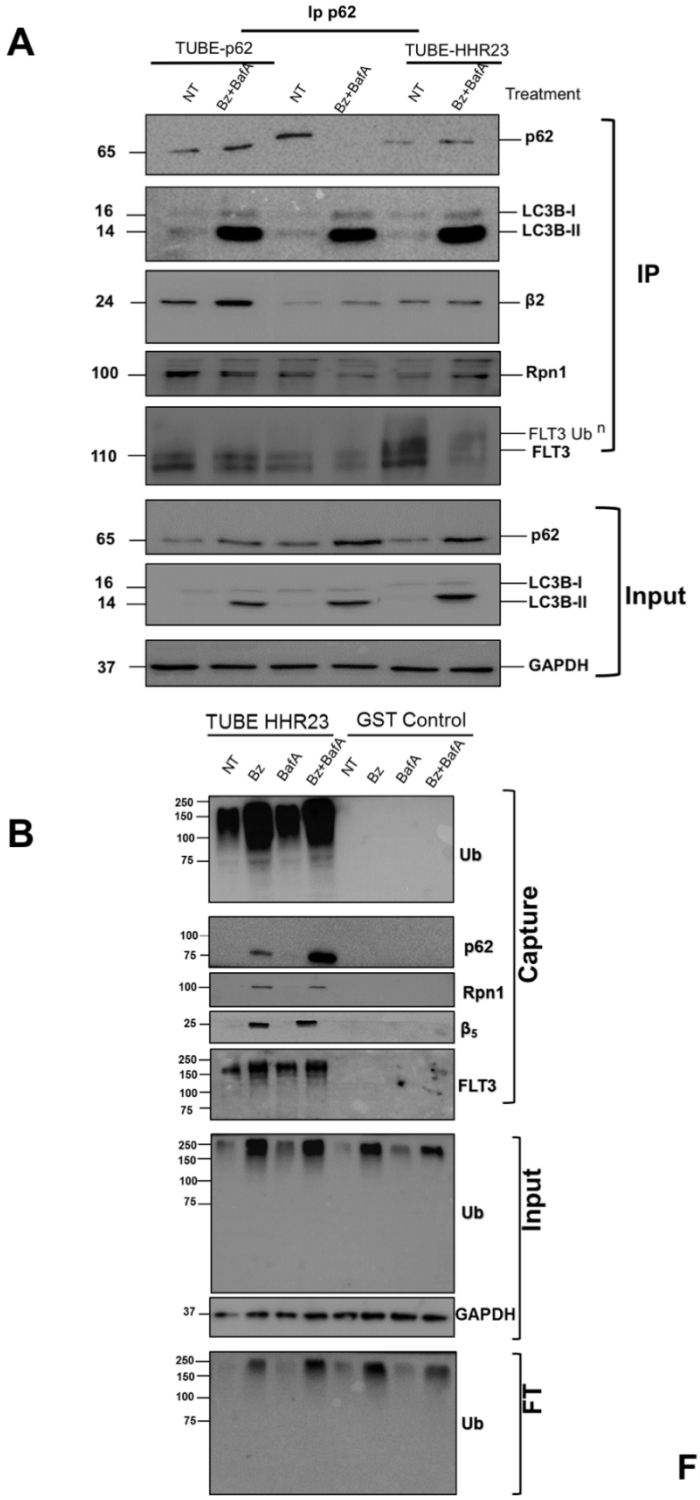

FIGURE 3

feb4_12950_f3.tiff

FEBS Open Bio (2020) © 2020 The Authors. Published by FEBS Press and John Wiley & Sons Ltd.

Accepted Article

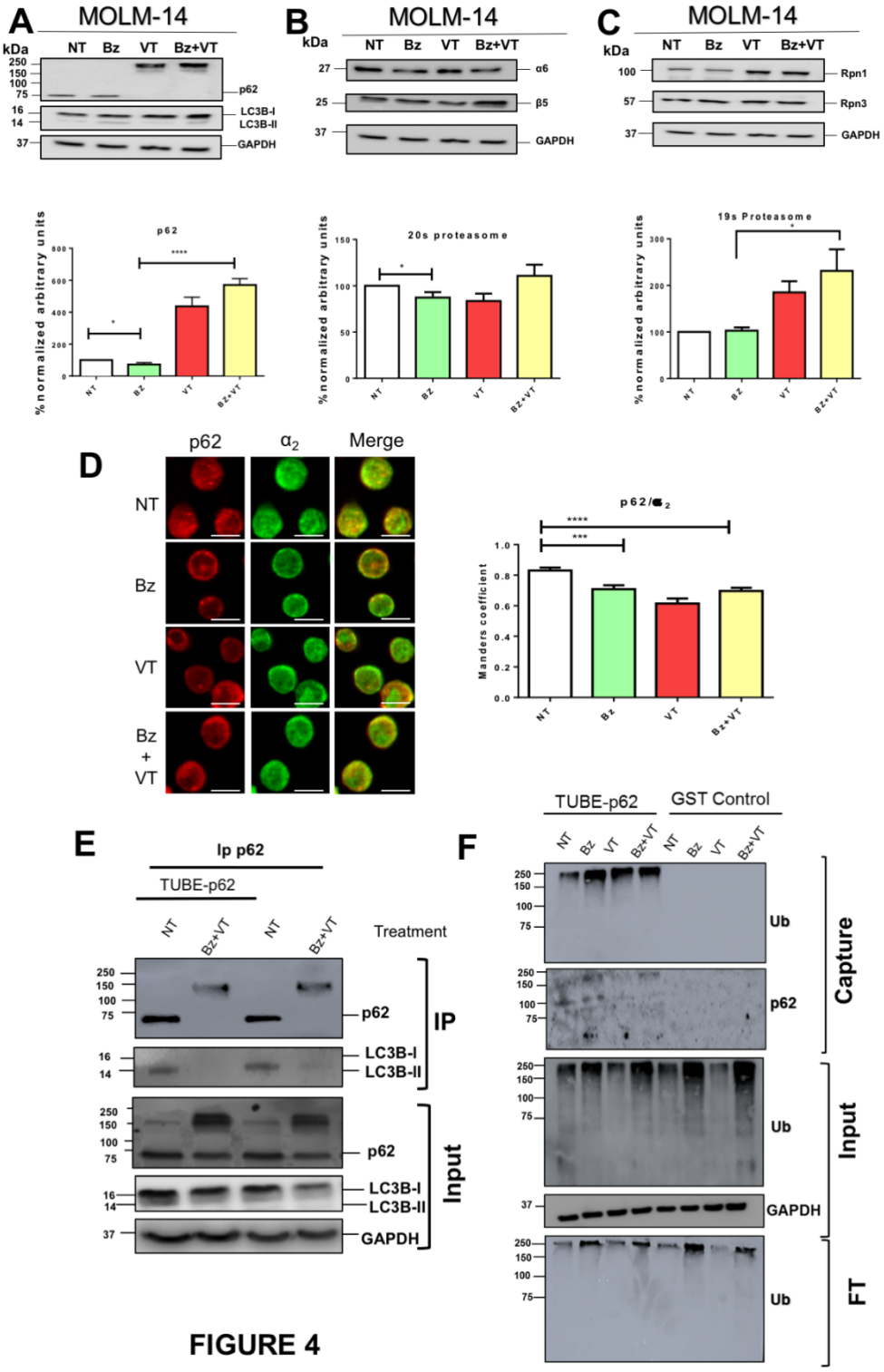

FIGURE 4

feb4_12950_f4.tiff

FEBS Open Bio (2020) © 2020 The Authors. Published by FEBS Press and John Wiley & Sons Ltd.

Accepted Article

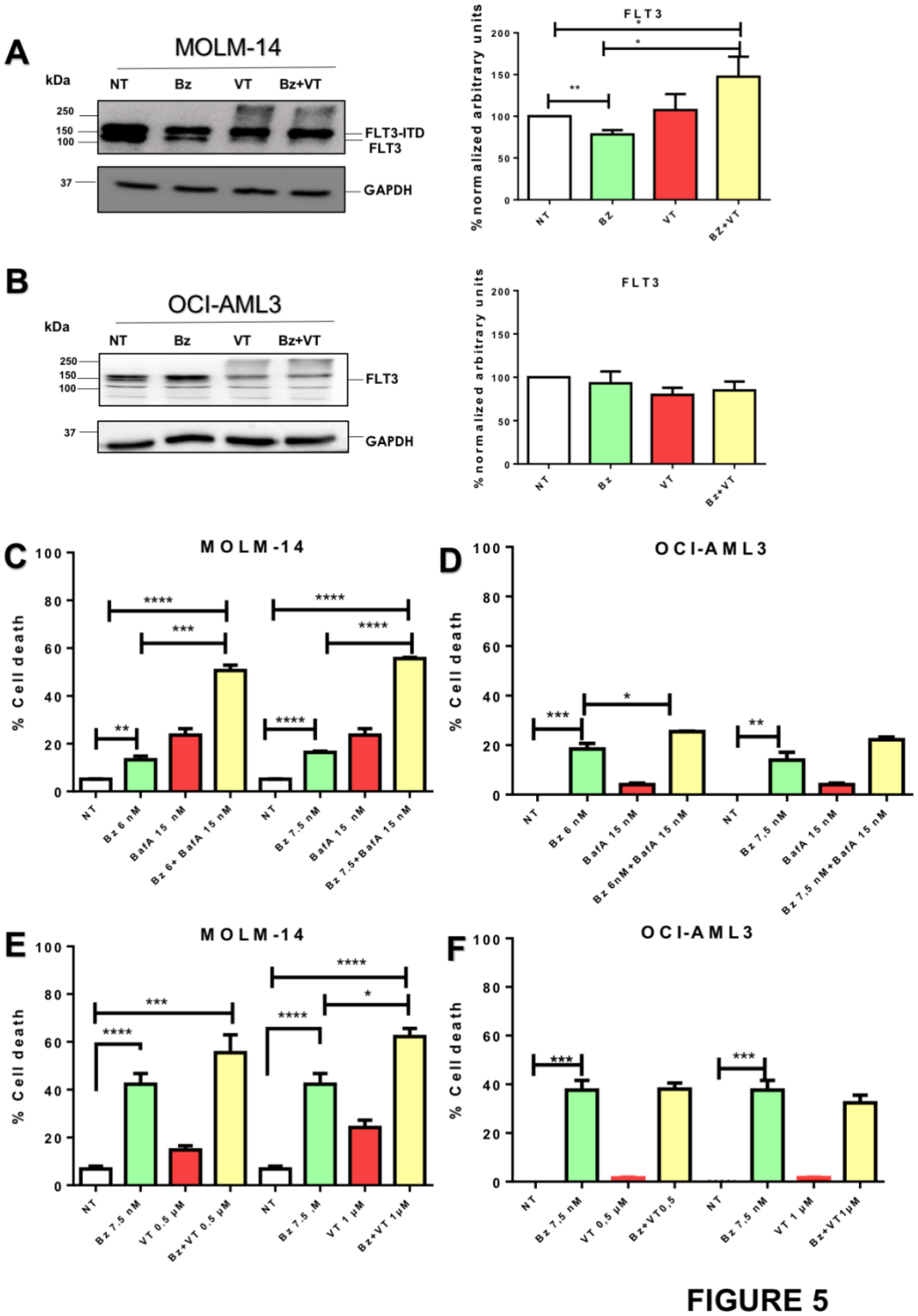

FIGURE 5

feb4_12950_f5.tiff

FEBS Open Bio (2020) © 2020 The Authors. Published by FEBS Press and John Wiley & Sons Ltd.

Accepted Article

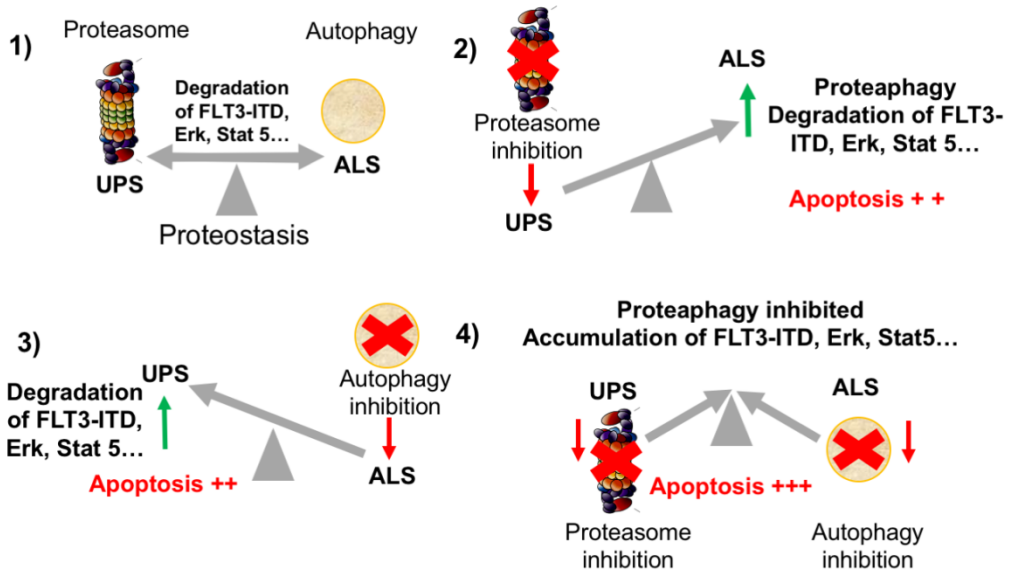

FIGURE 6

feb4_12950_f6.tiff

FEBS Open Bio (2020) © 2020 The Authors. Published by FEBS Press and John Wiley & Sons Ltd.